On-chip waveguide resonator with metallic mirrors

Steve Zamek,* Amit Mizrahi, Liang Feng, Aleksandar Simic, and Yeshaiahu Fainman

Department of Electrical and Computer Engineering, University of California, San Diego, 9500 Gilman Drive, La Jolla, California 92093, USA

**Corresponding author: szamek@ucsd.edu*

Received December 2, 2009; revised December 29, 2009; accepted January 2, 2010; posted January 20, 2010 (Doc. ID 120689); published February 12, 2010

We introduce an optical microresonator consisting of a planar waveguide terminated by metallic mirrors. The resonator was fabricated on a silicon-on-insulator platform, and its optical performance was theoretically and experimentally investigated. The demonstrated device had dimensions of 200 μm $\times$ 40 μm and exhibited a quality factor of about 1000 and a free-spectral range of about 8 nm. Application to high-throughput, label-free biochemical sensing is considered, and optimization with respect to the surface sensitivity is carried out. The optimized sensitivity makes it possible to detect subnanometer layers of molecules adsorbing to the surface of the resonator. © 2010 Optical Society of America

OCIS codes: 230.5750, 130.6010, 280.1415, 130.2790, 230.7400, 230.4040.

During the past decades optical microcavities found a large variety of applications in the fields of communications, display technologies, and biochemical sensing [1–3]. Realization of these devices using silicon-on-insulator (SOI) material platform will take advantage of the existing low-cost microelectronics manufacturing, making it particularly appealing for various applications of future optoelectronic systems. Aside from the numerous applications in silicon photonics, optical microcavities are strong candidates for the replacement of fluorescence-based arrays in biochemical sensing, thereby reducing time and cost of drug development, environment monitoring, and medical diagnostics [3]. In this regard, planar resonators allow dense integration of multiple devices on an SOI platform and are therefore especially suitable for chip-scale high-throughput biochemical sensor arrays. Such resonators can be constructed using distributed Bragg reflectors [4] or photonic crystals [5], or simply by cleaved waveguide facets.

In this Letter, we introduce an on-chip resonator made of a silicon waveguide terminated with metallic mirrors, and a grating coupler to allow excitation of the guided modes from free space, as shown in Fig. 1(a). Such mirrors have the benefit of high reflectivity for all transverse waveguide modes at an arbitrary wavelength. As a proof of concept we fabricated a 40-μm-long resonator, which exhibited a quality factor (Q) of about 1000, and a free spectral range (FSR) of 8.1 nm. Application of this resonator to label-free biochemical sensing is considered, and its surface sensitivity to adsorption of molecules (e.g., proteins) is investigated and optimized. The resulting ultrahigh sensitivity enables detection of a subnanometer monolayer of molecules, which is comparable to large grating couplers [6,7], thus allowing their miniaturization.

The resonator, shown in Fig. 1(a), consists of a thin silicon (Si) film ($n=3.48$) on top of a silicon dioxide (SiO_2) substrate ($n=1.46$). Aluminum (Al) mirrors are inserted into an Si waveguide, creating a resonator for the modes propagating along the x axis. A grating is patterned onto the Si guiding layer to facilitate excitation of the guided modes from free space. Provided that the y dimension of the resonator is sufficiently large, a simpler 2D model may be adopted, as shown in Fig. 1(b).

The resonator modes satisfy two phase relations for the optical field: (1) the dispersion relation of a slab waveguide given by

$$\beta = k_0 n_{\mathrm{eff}}(\lambda), \tag{1}$$

where β is the propagation constant of the waveguide mode; k_0 is the free-space wave number, corresponding to wavelength λ; and $n_{\mathrm{eff}}(\lambda)$ is the dispersion relation of the waveguide, and (2) the longitudinal resonance imposed by the metallic mirrors, given by

$$\beta L = m\pi, \tag{2}$$

where L is the resonator length and m is an integer designating the longitudinal mode number.

To derive the FSR we represent the set of Eqs. (1) and (2) as curves in the $\beta-\lambda$ plane. The lowest waveguide modes, TE_0 and TM_0, are of special interest, since they exhibit higher confinement, higher reflectivity off the mirrors, and higher surface sensitivity [6]. Their dispersion relation, Eq. (1), is plotted in Fig. 2(a), assuming the thickness to be $d=250$ nm. The condition for a longitudinal resonance is shown by three dashed lines, assuming the resonator length to be $L=3$ μm for a lucid illustration. The intersection points correspond to the eigenmodes of the resonator, and the distance between them is the FSR, designated by $\Delta\lambda$ in Fig. 2(a). Linearization of the dispersion curve yields

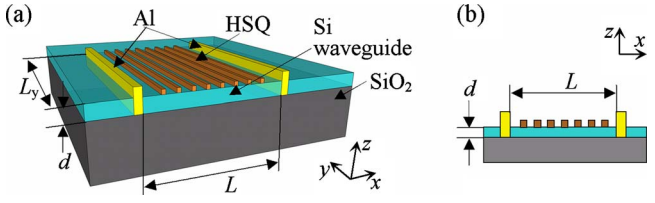

Fig. 1. (Color online) Resonator geometry: (a) Si slab waveguide with partial Al mirrors, (b) two-dimensional model.

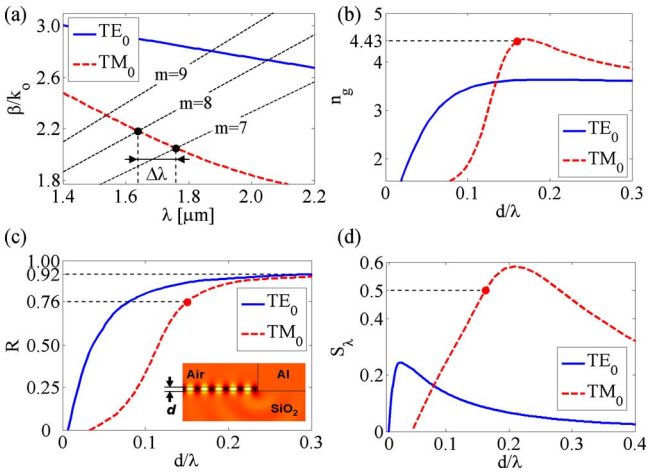

Fig. 2. (Color online) Resonator design considerations: (a) illustration of the two equations for the resonator modes, (b) group index as a function of waveguide thickness, (c) reflectivity of the partial Al mirror as a function of the waveguide thickness, and (d) Surface sensitivity for the proposed resonator. The red dots in (b)–(d) designate the fabricated resonator, and the inset in (c) shows finite-element method (FEM) simulation of $|H_y|$ for TM_0 mode in this case.

$$\Delta\lambda \approx \frac{\lambda^2}{2L}\left(n_g - \frac{\lambda}{2L}\right)^{-1}, \tag{3}$$

where $n_g = n_{\mathrm{eff}}(\lambda) - \lambda \partial n_{\mathrm{eff}}/\partial\lambda$ is the group index of the mode, shown in Fig. 2(b) as a function of d. The strong dependence of the FSR on the slab thickness is thus evident. For long cavities ($L \gg \lambda$), Eq. (3) simplifies to $\Delta\lambda \approx \lambda^2/2Ln_g$, which is a well-known result in the field of diode lasers [8].

The Q factor of the resonator in the 2D model may be expressed as $Q^{-1} = Q_m^{-1} + Q_g^{-1}$, where Q_m and Q_g correspond to the losses of the mirrors and the grating. To obtain Q_m, the reflectivity R of the Al mirror as a function of the slab thickness d is obtained using FEM, assuming $\epsilon = -235 - 42.5j$ as the permittivity of Al at $\lambda = 1.55$ μm, for time dependence of $\exp(j\omega t)$ [9]. The results are shown in Fig. 2(c) for the two lowest-waveguide modes, TE_0 and TM_0. Q_m is then given by [10]

$$Q_m = \frac{2\pi}{\lambda}\frac{Ln_g}{\ln(R^{-1})}, \tag{4}$$

such that Q_m is determined by both the group index and the reflectivity shown in Figs. 2(b) and 2(c), respectively.

The device was designed for operation with the TM_0 mode, which is favorable for biochemical sensing, as shown below. The resonator was fabricated on an SOI wafer with $d = 250$ nm thickness of the top Si layer, which corresponds to a group index $n_g = 4.43$ at $\lambda = 1550$ nm, and mirror reflectivity $R = 0.76$, as seen in Figs 2(b) and 2(c). The distance between the mirrors was chosen to be $L = 40$ μm, resulting in FSR = 7 nm, so that the finite grating length allows excitation of at least two resonances within the tuning range of the laser source, without changing the incidence angle. The corresponding quality factor is $Q_m = 2600$. A hydrogen silsesquioxane (HSQ) e-beam resist was used to create a grating with a period of 600 nm, whose (−1) diffraction order was used to excite TM_0 mode of the waveguide from free space. The Q factor due to the radiation losses of the grating ($n = 1.36$) is found from FEM simulations to be $Q_g \approx 3000$. The total Q factor of the resonator is calculated to be about 1400. The y dimension of the resonator was chosen to be $L_y = 200$ μm, so that the diffraction losses in the $x-y$ plane (see Fig. 1) do not significantly degrade this value of Q.

The fabrication consisted of three major steps. First, PMMA was used as an etch mask to define the mirrors on the SOI wafer. Next, reactive-ion etching was performed, followed by e-beam evaporation of Al with a consecutive lift-off, forming a waveguide terminated with Al mirrors. Finally, a grating was created by patterning HSQ resist on top of the resonator. Microscope and SEM micrographs of the fabricated device are shown in Fig. 3.

To characterize the performance of the resonator we used a tunable cw laser with a wavelength range of 1520 to 1570 nm. A beam with a diameter of 0.5 mm was incident upon the resonator at an angle of $21 \pm 1°$ to the normal through a polarizer set to excite the TM_0 mode of the waveguide. An objective with magnification of 10× was used to image the resonator onto a detector. The power reflected off the resonator as a function of the wavelength was recorded with a power meter, as shown by the dots in Fig. 4. The fluctuations seen in the data are due to reflections from the back facet of the chip and can be easily suppressed. The reflection spectrum exhibits typical asymmetrical resonant line shapes [7,11,12]. The data was fitted to a sum of Fano line shapes superimposed on a linear background. The result is shown in Fig. 4 by the solid curve, with the estimated resonance centers (λ) and linewidths (Γ) specified on the plot. The Q factors calculated from the fitted parameters are about 860 and 970 for the first and the second resonance, respectively. These are below the theoretical value ($Q \approx 1400$), obtained from the 2D model due to diffraction losses in the resonator plane and mirror imperfections. Significantly higher Q factors are feasible for the same resonator size with TE mode, thicker Si waveguide, and improvement of the mirror quality.

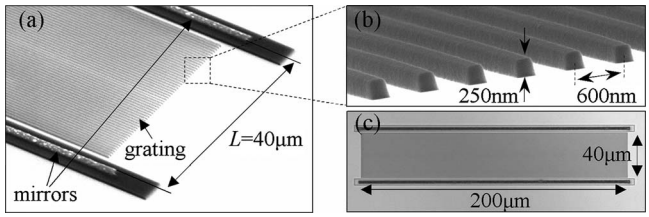

Fig. 3. Fabricated device. (a) Scanning-electron-microscope (SEM) micrograph of the resonator, showing the mirrors and the grating on top of a Si waveguide. The mirrors were coated with HSQ resist to prevent their oxidation. (b) High-magnification SEM micrograph showing the grating profile. (c) Micrograph of the entire resonator obtained with an optical microscope.

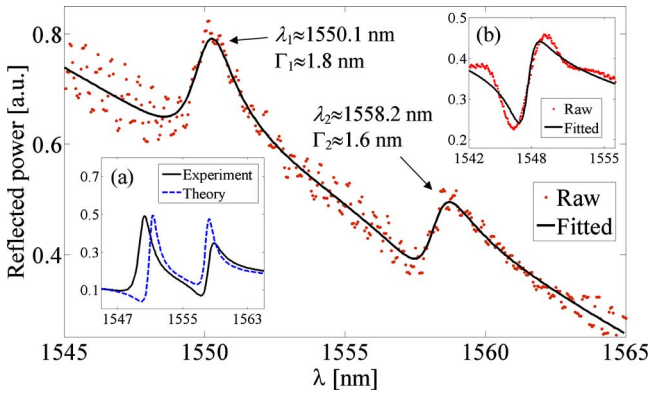

Fig. 4. (Color online) Experimental results: measured reflection spectrum (red dots) and the fitted model (solid black). Inset (a) shows comparison of the experimental results (solid black) with the simulated 2D model (dashed blue) reflection spectrum. Inset (b) shows a measured reflection spectrum of a large grating with no mirrors.

Both experimental and FEM simulated results were fitted to the above-mentioned model, and the linear background was removed from both for comparison. The two reflection spectra with their fitted model parameters are shown in inset (a) of Fig. 4. The experimental FSR (8.1 nm) differs from the one predicted by the 2D model (7 nm), due to an out-of-plane diffraction by the grating. We also fabricated a 200 μm $\times$ 200 μm grating, with the same profile as in the resonator. Its reflection spectrum is shown in inset (b) of Fig. 4. The small resonator exhibits Q factors higher than the one of the large grating, which is about 740, showing a clear benefit of the metallic mirrors.

We next consider application of the proposed microresonator to label-free biochemical sensing. It is established above that the proposed microresonator exhibits Q factors as high as those of larger gratings. We show below that this miniaturization is possible without a compromise in the surface sensitivity. Adsorption of a layer of biochemical molecules with thickness h onto the surface of the resonator results in a shift in the resonant wavelength. The surface sensitivity $S_\lambda \equiv \partial\lambda/\partial h$ is obtained by assuming $n_{\text{eff}} = n_{\text{eff}}(\lambda, h)$ in Eqs. (1) and (2) and differentiating them with respect to h,

$$S_\lambda \equiv \frac{\partial\lambda}{\partial h} = \lambda \frac{\partial n_{\text{eff}}}{\partial h} n_g^{-1}. \quad (5)$$

Here, $\partial n_{\text{eff}}/\partial h$ is the sensitivity of the effective index of the guided modes in an infinite slab waveguide [6]. The sensitivity of the resonator, S_λ, is shown in Fig. 2(d), assuming an adlayer with a refractive index of 1.45 adsorbing onto the surface of the resonator from water ($n = 1.33$). For our setup, the signal-to-noise ratio is sufficiently high (>30 dB), and the detection limit is given by the wavelength repeatability of the tunable laser source [13]. With the current repeatability of $\delta\lambda = 15$ pm, and maximum sensitivity of $S_\lambda \approx 0.6$, the minimum variation in the thickness of an adlayer that can be detected is $\Delta h = 2\delta\lambda/S_\lambda = 50$ pm. This is 2 orders of magnitude smaller than the typical thickness of protein monolayers and corresponds to 3.3 ng/cm^2 surface mass coverage [14]. Such sensitivity is appealing not only for biochemical sensing but also for environmental monitoring, where detection of extremely small molecules may be desired. In practice, the presence of the grating will decrease the actual surface sensitivity of the resonator, depending on the grating's duty cycle, such that in our device this decrease is by a factor of about 1.9.

In conclusion, we presented a novel type of chip-scale resonators, formed by a planar dielectric waveguide terminated with metallic mirrors. The simplified 2D model for such a resonator was developed and predicted the Q factor and FSR in good agreement with the experimental results. The proposed mirrors exhibit low spectral sensitivity, high reflection for arbitrary polarization, and different transverse waveguide modes. The resonator was optimized to enable detection of the smallest molecules adsorbing to its surface. The ultracompact size of the metallic mirrors and the high fabrication tolerances are promising for future chip-scale high-throughput label-free biochemical sensor arrays, as well as other applications in silicon photonics.

This work was supported by the Defense Advanced Research Projects Agency (DARPA), the National Science Foundation (NSF), and Center for Integrated Access Networks Engineering Research Center.

References

1. K. Vahala, Nature **424**, 839 (2003).
2. V. V. Doan and M. J. Sailor, Science **256**, 1791 (1992).
3. M. Cooper, Nat. Rev. Drug Discovery **1**, 515 (2002).
4. D. T. H. Tan, K. Ikeda, and Y. Fainman, Opt. Lett. **34**, 1357 (2009).
5. H.-C. Kim, K. Ikeda, and Y. Fainman, Opt. Lett. **32**, 539 (2007).
6. K. Tiefenthaler and W. Lukosz, J. Opt. Soc. Am. B **6**, 209 (1989).
7. J. Schmid, W. Sinclair, J. García, S. Janz, J. Lapointe, D. Poitras, Y. Li, T. Mischki, G. Lopinski, P. Cheben, A. Delâge, A. Densmore, P. Waldron, and D. Xu, Opt. Express **17**, 18371 (2009).
8. M. I. Nathan, A. B. Fowler, and G. Burns, Phys. Rev. Lett. **11**, 152 (1963).
9. E. D. Palik, ed., *Handbook of Optical Constants of Solids* (Academic, 1985).
10. A. Yariv, *Quantum Electronics* (Wiley, 1989), p. 147.
11. S. Glasberg, A. Sharon, D. Rosenblatt, and A. A. Friesem, Opt. Commun. **145**, 291 (1998).
12. S. Fan, W. Suh, and J. Joannopoulos, J. Opt. Soc. Am. A **20**, 569 (2003).
13. G. M. Hwang, L. Pang, E. H. Mullen, and Y. Fainman, IEEE Sens. J. **8**, 2074 (2008).
14. J. A. De Feijter, J. Benjamins, and F. A. Veer, Biopolymers **17**, 1759 (1978).